Journal Pre-proofs

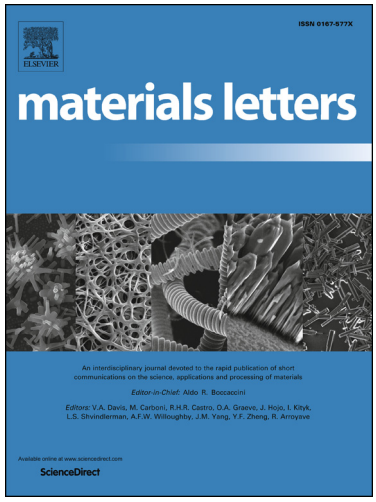

Evolution of microstructures and divorced eutectic TiC formed during solidification of the wear-resistant steel

Gang Du, Feng Liu, Jian-bing Li

PII: S0167-577X(20)30111-7
DOI: https://doi.org/10.1016/j.matlet.2020.127406
Reference: MLBLUE 127406

To appear in: *Materials Letters*

Received Date: 18 December 2019
Revised Date: 5 January 2020
Accepted Date: 21 January 2020

Please cite this article as: G. Du, F. Liu, J-b. Li, Evolution of microstructures and divorced eutectic TiC formed during solidification of the wear-resistant steel, *Materials Letters* (2020), doi: https://doi.org/10.1016/j.matlet.2020.127406

Evolution of microstructures and divorced eutectic TiC formed during solidification of the wear-resistant steel

Gang Du, Feng Liu*, Jian-bing Li*

State Key Laboratory of Solidification Processing, Northwestern Polytechnical University, Xi'an 710072, PR China

*Corresponding author. E-mail address: singsundu@sina.com, liufeng@nwpu.edu.cn.

A B S T R A C T

The effect of cooling rate on the microstructure and TiC precipitation of TiC-reinforced wear-resistant steel was investigated by different casting techniques. Thermodynamic and solute segregation modeling was performed to determine the evolution of TiC fraction in wear-resistant steel after rapid solidification. The evolution of TiC fraction due to solute segregation within the framework of Clyne–Kurz (C-K) model was examined. The model prediction is consistent with the experimental results.

Keywords: Solidification; Divorced eutectic; TiC; Microstructure; Wear-resistant steel

1. Introduction

As transition metal carbide, TiC is characterized by its excellent properties such as very high melting point and hardness [1,2]. These properties have led to their wide applications as important precipitates for strengthening steels [3,4]. The volume fraction, particle size and distribution of the reinforcing phase are significant for improving the mechanical properties [5,6]. To obtain the desired wear resistant properties and mechanical strength of steels, it is important to control the volume fraction of TiC [7]. As it is known, the inevitable solute segregation occurred in non-equilibrium solidification process enriches the solute in liquid, and influence the amount of eutectic and other phases [8]. Quantitative prediction of microsegregation is complicated by the difficulties in accounting for eutectic and secondary phase formation in steel. Within the past decades, correspondingly various analytical models were developed to predict solute redistribution and related phenomena [9-14]. Among these microsegregation models, the Clyne–Kurz model is considered to be the most popular one. However, previous works have the disadvantage that a constant partition coefficient must be assumed.

It is known that cooling rate plays an important role in the precipitation behavior during solidification of steels [15]. When the cooling rate becomes larger, the growth velocity increases to a point where the solute trapping must be taken into account. Under this condition, the local equilibrium was ruled out and the partition coefficient of solute elements at the solid-liquid (S/L) interface could not be kept constant any more, which is one of the main features of non-equilibrium solidification. The present work focuses on investigating the evolution characteristics of microstructure and TiC precipitation of TiC-reinforced wear-resistant steel via conventional casting and spray casting.

2. Thermodynamic Calculation on Solidification Path and Segregation Behavior

The chemical composition of steel is C 0.35, Al 0.23, Ti 3.0, Si 0.5, Mn 0.35, Cr 0.68, Mo 0.28, Ni 0.51 (wt%) and Fe as balance. The Gulliver–Scheil model was used to predict non-equilibrium solidification of the experimental steel by Thermo-Calc software, and the calculation result is shown in Fig. 1a. It can be seen that the corresponding solidification path is L → L+δ → L+δ+TiC → δ+TiC; i.e., first, δ ferrite is formed in liquid, then a secondary phase TiC is formed when the solid fraction reaches 0.04. Finally, the liquid transforms into a mixture of ferrite and TiC.

Fig. 1b represents the main element segregation in liquid as a function of temperature calculated by using Thermo-Calc software. Combined with Fig. 1a, it can be found that the secondary phase TiC appears once the liquid composition reaches a critical value. The obtained critical value of liquid composition is C 0.34, Al 0.20, Ti 3.25, Si 0.57, Mn 0.38, Cr 0.69, Mo 0.30, Ni 0.56 (wt%) and Fe as balance. The phase transformation occurring at this critical composition is calculated by using Thermo-Calc software, shown in Fig. 1c. It can be seen that the precipitation of TiC is attributed to a eutectic reaction L → $(\delta+TiC)_{eutectic}$ and the solidification path can be expressed as L → L+δ → L+δ+$(\delta+TiC)_{eutectic}$→ δ+$(\delta+TiC)_{eutectic}$.

3. Modeling of the eutectic fraction

As solute is generally rejected into the liquid, microsegregation is resulted from solute redistribution and solute segregation during solidification [16]. Assuming parabolic growth for interface advance velocity (V) with increasing

time (i.e., $V = \frac{\lambda_2}{4f \cdot t_f}$), solute redistribution equation can be expressed as [17]

$$C_L = C_0\left[1-(1-2Ak)f\right]^{(k-1)/(1-2Ak)} \quad (1)$$

where *f* is the solid fraction, C_L the solute concentration at the S/L interface, C_0 the initial solute concentration and

$$A = 2\alpha\left(1-\exp\left(-\frac{1}{\alpha}\right)\right)-\exp\left(-\frac{1}{2\alpha}\right) \quad (2)$$

in which $\alpha = \frac{4D_s t_f}{\lambda_2^{\,2}}$ (3)

where D_s is the solute diffusivity in the solid, λ_2 is the secondary dendrite arm spacing (SDAS), and the local solidification time t_f can be expressed as [18]

$$t_f = \Delta T / R \quad (4)$$

where $^{\triangle}$T and *R* are the temperature range of solidification and cooling rate, respectively. To calculate the solute concentration of the liquid at the S/L interface during non-equilibrium solidification, the non-equilibrium partition coefficient is not known a priori. According to the solute-trapping model proposed by Sobolev [19], the non-equilibrium partition coefficient (k) can be expressed as

$$k = \frac{V/V_{\mathrm{DI}} + k_{\mathrm{e}}}{V/V_{\mathrm{DI}} + 1} \quad (5)$$

with k_e as the equilibrium partition coefficient and V_{DI} the interface diffusive speed. The enrichment of solute in the interdendritic region leads to the fomation of eutectic phase during solidification process.

Zhang [18] proposed a segregation model for rapid solidification that assumes incomplete diffusion in the liquid. In this model, the amount of solute enrichment (S_e) can be expressed as [18]

$$\mathrm{S_e} = \frac{\lambda_2}{2}\cdot f_{eut}(C_L - C_e) \quad (6)$$

where f_{eut} represents the fraction of nonequilibrium eutectic. The amount of solute depletion (S_d) in the solid can be given as

$$\mathrm{S_d} = C_0\frac{\mathrm{D_L}(1-k)}{Vk} \quad (7)$$

where D_L is the solute diffusivity in the liquid and V is the local interface advance velocity. As the amount of solute enriched in the liquid is equal to the amount of solute depletion in the solid, i.e., $S_e = S_d$. Combined with Eqs. (6) and (7), the eutectic fraction f_{eut} can be derived as

$$f_{eut} = \frac{1 - f(1-k)}{fk} \cdot \frac{2D_L}{\lambda_2 V} \quad (8)$$

4. Experimental procedure

Samples were produced by conventional casting and spray casting processes representing different cooling effect ranges. In conventional casting, two steel bars were melted and heated to 1843 K by induction coils and then cooled to 1273 K at rates of 0.2 and 11 K/s, respectively. In the case of the spray casting process, steel bars were melted and heated to 1843 K by induction coils and the melt was sprayed in the vacuum chamber followed by cooling to 1273 K at rates of 162 and 267 K/s. After the experiments, each sample was sectioned along the radial direction and metallographically prepared. The specimens were studied by optic microscopy (OM) and scanning electron microscopy (SEM). The SDAS and the TiC fraction were measured and calculated according to the micrographs.

5. Results and discussions

Fig. 2a-d shows the OM microstructure of the experimental steel at different solidification cooling rate. For a very low cooling rate (0.2 K/s), the sample shows cross morphology and coarse dendritic microstructures. With the increase of cooling rate to 11 and 162 K/s, dendrite arm spacings decrease and dendritic refinement occurs. Finally, under the ultra-high solidification rate 267 K/s, a superfine cellular microstructure with fewer side branches is obtained. The SDAS of samples were measured to be 38.57, 17.87, 6.81 and 3.83 μm respectively, and the relationship between λ_2 and $R^{-1/3}$ can be expressed as $\lambda_2 = 23.50R^{-1/3}$. Fig. 2e-f shows the typical SEM microstructures of the experimental steel. EDS analysis shows that the interdendritic TiC precipitate is enriched in Ti and C, as shown in Fig. 2i and j. Fig. 2k shows the XRD pattern of the solidified microstructure in TiC-reinforced wear-resistant steel, which confirms that TiC and ferrite are contained in the experiment steel. As it can be seen, the volume fraction of TiC precipitates decreases

with the increase of cooling rate. Moreover, the divorced eutectic morphology characterized by the isolated morphology of TiC precipitate is observed in the experimental steel.

Fig. 3a shows the change of fractions of the remaining liquid, TiC and δ phases with decreasing temperature calculated by Thermo-Calc. It can be seen that the fraction of remaining liquid decreases and the fraction of TiC and ferrite phase increases with decreasing temperature. As the eutectic phase is composed of TiC and δ phase, the change of fractions of eutectic phase with temperature can be obtained. Then the relationship between TiC fraction and eutectic fraction can be determined as $f_{\mathrm{TiC}} = 0.02 \cdot f_{eut}$. Table 1 lists the values of the parameters adopted in the present modeling. Integration of the Eqs. (1)-(5), (8) and Table 1 leads to the value of f_{TiC} under different cooling rate, as shown in Fig. 3b. Fig. 3b compares the predicted TiC fractions with the experimental data. As shown in Fig. 3b, the fraction of TiC decreases with increasing cooling rate. The resulting analytical predictions by the current model can be applied in the steel industry to predict TiC fraction during solidification of wear-resistant steel.

6. Conclusion

The model for evolution of TiC fraction due to solute segregation was constructed with the use of thermodynamic modeling and formal combination of Clyne–Kurz model. With the increase of cooling rate in the range from 0.2 K/s to 267 K/s, the S/L interface experiences dendritic and superfine cellular morphologies. The formation of the interdendritic TiC precipitate in the experiment steel was attributed to the eutectic reaction during solidification, as $L \rightarrow (\delta+TiC)_{eutectic}$, but it exhibited a divorced eutectic structure. The general character of the present model permits to predict the fraction of divorced eutectic phase formed upon solidification of similar steel.

Conflicts of Interest:

The authors declare no conflict of interest.

Acknowledgements

This work was financially supported by the National Key R&D Program of China (No. 2017YFB0305101).

References

[1] L. Sun, J.S. Pan, Mater. Lett., 51 (2001) 270-274.

[2] S. Kang, Comprehensive Hard Materials, Elsevier Ltd., New York, 2014.

[3] D. Grzesiak, B. AlMangour, M. Krawczyk, M.S. Baek, K.A. Lee, Mater. Lett. 256 (2019) 1-4.

[4] D. Grzesiak, B. AlMangour, M. Krawczyk, M.S. Baek, K.A. Lee, Mater. Lett. 256 (2019) 1-4.

[5] B. AlMangour, D. Grzesiak, J.M.Yang, Mater. Des. 104 (2016) 141-151.

[6] B. AlMangour, D. Grzesiak, J.M.Yang, Mater. Des. 96 (2016) 150-161.

[7] Z.C. Luo, J.P. Ning, J. Wang, K.H. Zheng, Wear 432–433 (2019) 1-10.

[8] T. Antonsson, H. Fredriksson, Metall. Mater. Trans. B 36B (2005) 85-96.

[9] H.D. Brody, M.C. Flemings, Trans. TMS-AIME 236 (1966) 615-24.

[10] T.W. Clyne, W. Kurz, Metall. Trans. A 12A (1981) 965-971.

[11] A. Turkeli, IOP Conf. Ser.: Mater. Sci. Eng. 117 (2016) 1-6.

[12] B. Thomas, D. Dominique, R. Bernard, T. Guillaume, K. Jacob, R. Vincent, Z. Julien, Materials 11 (2018) 1107-1252.

[13] A. Howe, Ironmak. Steelmak. 38 (2011) 534-539.

[14] J.G. Jung, Y.H. Cho, J.M. Lee, H.W. Kim, K. Euh, Calphad 64 (2019) 236-247.

[15] G. Du, J. Li, Z.B. Wang, Metall. Mater. Trans. B 48 (2017) 2873-2890.

[16] V.R. Voller, C. Beckermann, Metall. Mater. Trans. A 30A (1999) 2183-2189.

[17] T.W. Clyne, W. Kurz, Metall. Mater. Trans. A 12 (1981) 965-971.

[18] H.Q. Hu, Fundamentals of Metal Solidification, China Machine Press, Beijing, 2000.

[19] S.L. Sobolev, Phys. Rev. E 55 (1997) 6845-6854.

[20] C.Y. Meng, B.G. Thomas, Metall. Mater. Trans. B 34 (2003), 685-705.

[21] P.J. Alberry, C.W. Haworth, Met. Sci. 8 (1974) 407-412.

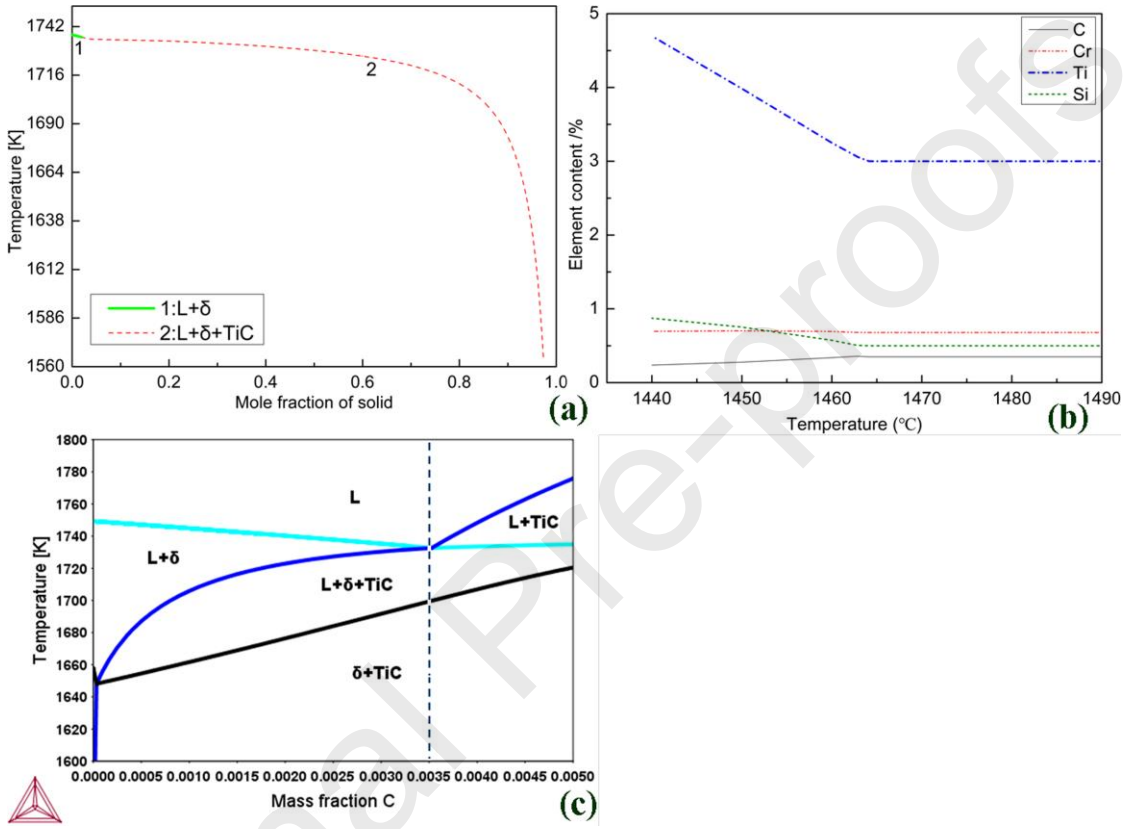

Fig. 1. (a) Calculated non-equilibrium solidification process for the experimental steel using the Scheil-Gulliver model in Thermo-Calc. (b) Calculated main element segregation in liquid as a function of temperature. (c) Predicted phase diagram at the critical liquid composition.

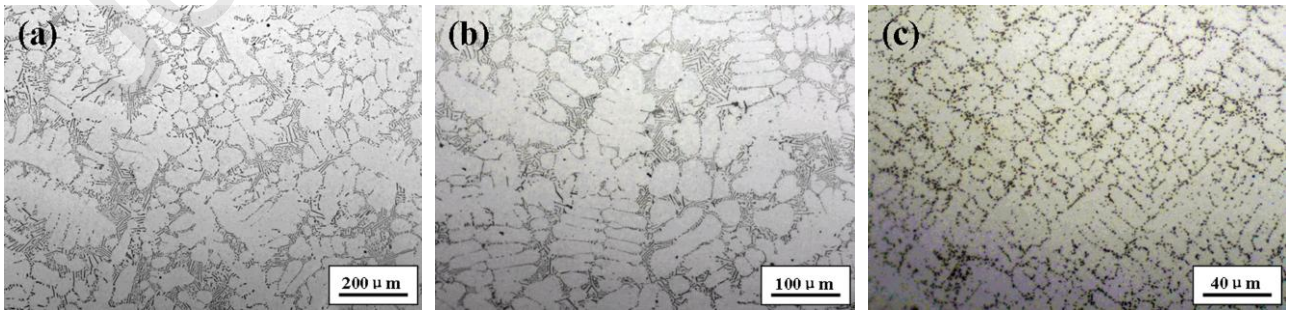

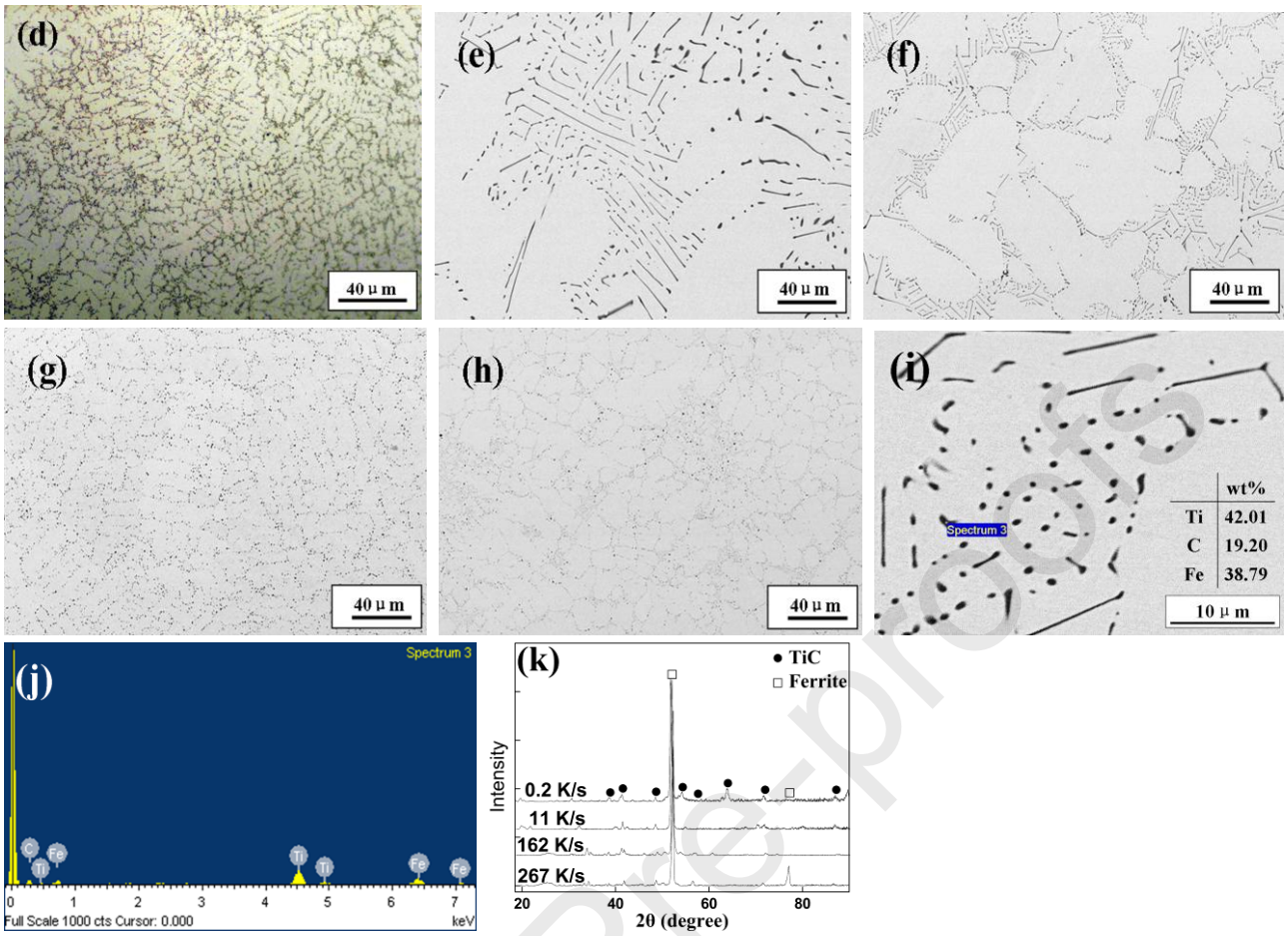

Fig. 2. (a-d) OM and (e-h) SEM images of microstructure evolution of the steel as a function of cooling rate: (a, e) 0.2 K/s; (b, f) 11 K/s; (c, g) 162 K/s; (d, h) 267 K/s and (i) Chemical composition and (j) EDS source profile of the typical TiC precipitate observed in the current study and (k) XRD profile of the TiC-reinforced wear-resistant steel.

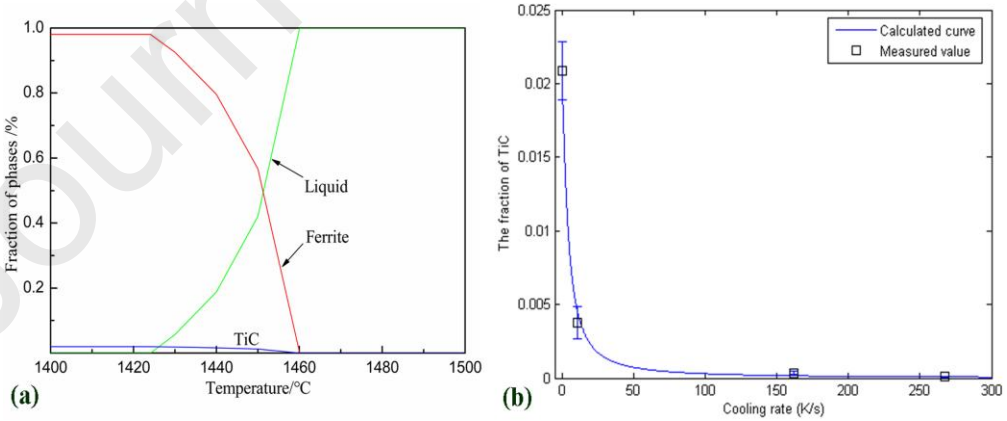

Fig. 3. (a) Change of phase fractions with temperature during eutectic reaction. (b) Comparison of the predicted TiC fractions with the measured ones in solidification of the experiment steel under different cooling rates.

Table 1 Values of the parameters adopted in the present modeling [20, 21].

Parameter	Ti	Reference

Initial solute concentration, C_0 (wt%)	3.0	
Equilibrium distribution coefficient, k_0	0.38	[20]
Solute diffusion coefficient, D_L (cm^2/s)	7.3×10^{-5}	[21]
Solute diffusion coefficient, D_S (cm^2/s)	1.2×10^{-7}	[20]
Liquidus, T_L (℃)	1514	
Solidus, T_S (℃)	1479	

Highlights

The solid/liquid interface experiences dendritic and superfine cellular morphologies with the increase of cooling rate

The formation of the interdendritic TiC was attributed to the eutectic reaction during solidification

The interdendritic TiC phase exhibited a divorced eutectic structure

The general character of the present model permits to predict TiC precipitation during solidification of wear-resistant steel

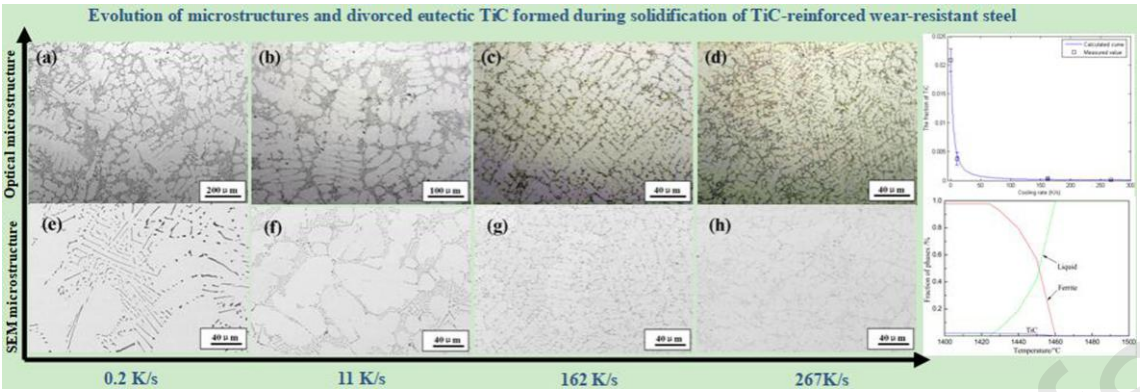

CRediT author statement

Gang Du: Conceptualization, Methodology, Writing-Original draft preparation. Feng Liu: Project administration, Funding acquisition. Jian-bing Li: Visualization, Investigation.